Neural sirtuin 6 (Sirt6) ablation attenuates somatic growth and causes obesity

Bjoern Schwer[a], Bjoern Schumacher[b], David B. Lombard[a,1], Cuiying Xiao[c], Martin V. Kurtev[d], Jun Gao[e], Jennifer I. Schneider[b], Hua Chai[a], Roderick T. Bronson[f], Li-Huei Tsai[e,g], Chu-Xia Deng[c], and Frederick W. Alt[a,2]

[a]Howard Hughes Medical Institute, Program in Cellular and Molecular Medicine, Children's Hospital, Immune Disease Institute, Department of Genetics, Harvard Medical School, Boston, MA 02115; [b]Cologne Excellence Cluster for Cellular Stress Responses in Aging-Associated Diseases, Institute for Genetics, University of Cologne, 50674 Cologne, Germany; [c]Genetics of Development and Disease Branch, National Institute of Diabetes, Digestive and Kidney Diseases, National Institutes of Health, Bethesda, MD 20892; [d]Department of Neurology and Neurobiology, Harvard Medical School, Boston, MA 02115; [e]Picower Institute for Learning and Memory, Department of Brain and Cognitive Sciences, Howard Hughes Medical Institute, Massachusetts Institute of Technology, Cambridge, MA 02139; [f]Department of Pathology, Harvard Medical School, Boston, MA 02115; and [g]Stanley Center for Psychiatric Research, Broad Institute of Harvard University and Massachusetts Institute of Technology, Cambridge, MA 02142

Contributed by Frederick W. Alt, November 1, 2010 (sent for review October 4, 2010)

In yeast, Sir2 family proteins (sirtuins) regulate gene silencing, recombination, DNA repair, and aging via histone deacetylation. Most of the seven mammalian sirtuins (Sirt1–Sirt7) have been implicated as NAD$^+$-dependent protein deacetylases with targets ranging from transcriptional regulators to metabolic enzymes. We report that neural-specific deletion of sirtuin 6 (Sirt6) in mice leads to postnatal growth retardation due to somatotropic attenuation through low growth hormone (GH) and insulin-like growth factor 1 (IGF1) levels. However, unlike Sirt6 null mice, neural Sirt6-deleted mice do not die from hypoglycemia. Instead, over time, neural Sirt6-deleted mice reach normal size and ultimately become obese. Molecularly, Sirt6 deletion results in striking hyperacetylation of histone H3 lysine 9 (H3K9) and lysine 56 (H3K56), two chromatin marks implicated in the regulation of gene activity and chromatin structure, in various brain regions including those involved in neuroendocrine regulation. On the basis of these findings, we propose that Sirt6 functions as a central regulator of somatic growth and plays an important role in preventing obesity by modulating neural chromatin structure and gene activity.

Sirtuins have been linked to metabolic regulation, stress tolerance, and aging (1, 2). It is still unclear whether mammalian sirtuins function as longevity assurance factors; but they may have therapeutic potential for age-associated diseases (1). Seven mammalian sirtuins (Sirt1–Sirt7) are known and localize to various subcellular compartments (1, 2). Sirt6 is a chromatin-associated nuclear protein affecting DNA repair, telomere maintenance, gene expression, and metabolism (3–9). Sirt6-deficient (Sirt6$^{-/-}$) mice suffer from a severe, multisystemic phenotype and have a short lifespan (3, 4). This precludes studies of Sirt6 function in adult mice and makes it difficult to distinguish primary versus secondary consequences of Sirt6 loss. Postnatal growth retardation associated with low insulin-like growth factor 1 (IGF1) levels is a prominent feature of Sirt6$^{-/-}$ mice (4). Because brain homeostatic centers control somatic growth and IGF1 levels (10), and Sirt6 is highly expressed in the central nervous system (4, 11, 12), we hypothesized that loss of neural Sirt6 contributes to these aspects of the Sirt6-deficient mouse phenotype.

Results and Discussion

To circumvent the problem of early postnatal lethality of Sirt6$^{-/-}$ mice and to study the biological role of Sirt6 in the central nervous system, we generated neural-specific Sirt6 knockout mice (BS6^{ko}) by crossing mice carrying a conditional Sirt6 allele (6), in which exons 2 and 3 are flanked by *LoxP* sites, to Nestin-Cre (NCre) transgenic mice (13). BS6^{ko} mice showed efficient Sirt6 deletion, as determined at both DNA and protein levels, in the brain but not in other tissues (Figs. 1*A* and Fig. S1). Consistent with NCre-mediated deletion not occurring in the anterior pituitary (13, 14), Sirt6 expression in this organ was similar in BS6^{ko} and Sirt6 wild-type (WT) mice (Fig. 1*A*). BS6^{ko} mice appeared normal at birth and gross macroscopic and histological examination of 3-wk-old BS6^{ko} brains did not reveal any abnormalities (Fig. S2). However, at 4 wk of age, BS6^{ko} mice were significantly smaller (Fig. 1*B*) and weighed less (Fig. 1*C*) than littermate controls (Sirt6$^{+/+}$/NCre, Sirt6$^{+/+}$, Sirt6$^{c/+}$, or Sirt6$^{c/c}$; all hereafter referred to as WT). In contrast, no growth retardation occurred in Sirt6$^{c/+}$ mice containing the NCre allele (BS6^{het}) (Fig. 1 *C* and *D*). Growth retardation in BS6^{ko} occurred in both genders, but was more pronounced in males (Fig. 1*C*). These results demonstrate that neural Sirt6 inactivation is sufficient to cause growth retardation comparable to that observed in Sirt6$^{-/-}$ mice.

Unlike Sirt6$^{-/-}$ mice (3, 4), BS6^{ko} mice did not show progressive hypoglycemia; blood glucose levels were slightly lower but still within normoglycemic range in 3-wk-old BS6^{ko} mice (Fig. S3). Subsequently, BS6^{ko} mice gradually grew in size and weight and by 6–7 wk of age became indistinguishable from WT mice (Fig. 1*D*). To test whether reduced ability to compete for maternal resources during the postnatal period was a cause of growth retardation in BS6^{ko} mice, we performed cross-fostering experiments. Raising BS6^{ko} pups in the absence of WT pups did not rescue or alleviate the growth retardation phenotype (Fig. 1*E*). Furthermore, despite being small, BS6^{ko} pups were not physically impaired (Movie S1) and actually displayed slightly higher locomotor activity (Fig. S4). These results suggest that an intrinsic endocrine defect potentially causes growth retardation of BS6^{ko} mice.

Sirt6$^{-/-}$ mice routinely have low levels of IGF1 (4), a stable indicator of growth hormone (GH) secretion and, together with GH, the major regulator of postnatal growth (10). We measured IGF1 serum levels in 4-wk-old BS6^{ko} mice; similar to Sirt6$^{-/-}$ mice, BS6^{ko} had very low levels of circulating IGF1 (Fig. 2*A*). GH is secreted in pulsatile fashion by the pituitary in response to stimulation by hypothalamic growth hormone-releasing hormone (GHRH) (10). Albeit smaller, pituitaries from BS6^{ko} mice appeared grossly normal. Histological examination revealed that acidophils, which are mostly somatotrophs that produce GH (10), were present in the anterior pituitary; however, they were reduced in number and

Author contributions: B. Schwer, B. Schumacher, D.B.L., J.G., L.-H.T., and F.W.A. designed research; B. Schwer, B. Schumacher, D.B.L., M.V.K., J.G., J.I.S., and H.C. performed research; C.X. and C.-X.D. contributed new reagents/analytic tools; B. Schwer, B. Schumacher, D.B.L., J.G., R.T.B., L.-H.T., and F.W.A. analyzed data; and B. Schwer and F.W.A. wrote the paper.

Conflict of interest statement: F.W.A. and L-H.T. are members of the scientific advisory board of Sirtris Pharmaceuticals. However, the authors declare no competing financial interests.

Freely available online through the PNAS open access option.

[1]Present address: Department of Pathology and Institute of Gerontology, University of Michigan, Ann Arbor, MI 48109.

[2]To whom correspondence should be addressed. E-mail: alt@enders.tch.harvard.edu.

This article contains supporting information online at www.pnas.org/lookup/suppl/doi:10.1073/pnas.1016306107/-/DCSupplemental.

Downloaded by guest on December 7, 2021

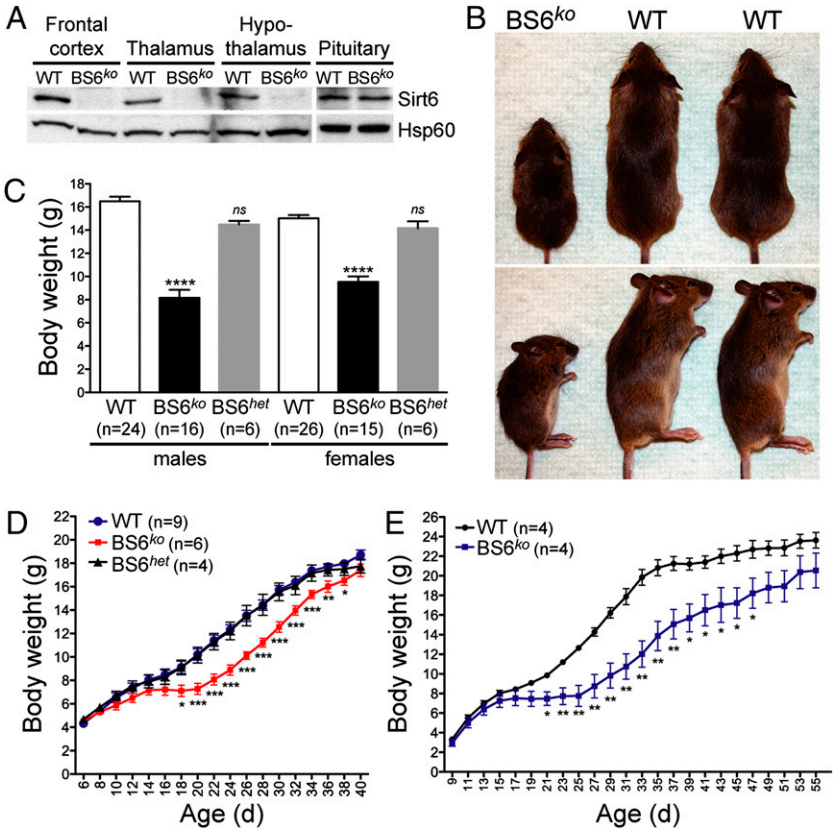

Fig. 1. Neural Sirt6 is required for normal postnatal somatic growth. (*A*) Neural-specific deletion of Sirt6. Immunoblot analysis of Sirt6 expression in various brain regions and pituitary from WT or BS6^{ko} mice. (*B*) Growth retardation in BS6^{ko} mice. Representative photographs of 4-wk-old male BS6^{ko} and WT littermates. (*C*) Average weights of 4-wk-old BS6^{ko}, BS6^{het}, and WT mice. (*D*) Growth curves of female BS6^{ko}, BS6^{het}, and WT mice. (*E*) Cross-fostering does not rescue growth retardation of BS6^{ko} mice. Significant differences (unpaired two-tailed *t* test for comparison of two groups; one-way ANOVA plus Bonferroni posttest for multiple comparisons) are indicated. $*P < 0.05$, $**P < 0.01$, $***P < 0.001$, $****P < 0.0001$; NS, not significant. Error bars denote SEM.

smaller in size than normal somatotrophs, with only a thin rim of cytoplasm (Fig. 2 *B* and *C*). Consistent with these observations, pituitaries from BS6^{ko} mice contained much less GH (Fig. 2*D*). GH deficiency appeared specific and not due to a generalized pituitary dysfunction because BS6^{ko} mice displayed normal levels of thyroid-stimulating hormone (TSH; Fig. S5). Whereas the specific cause of reduced somatotroph number and function remains to be determined, it does not appear to be due to a primary pituitary defect, because Sirt6 was not deleted in this organ. Furthermore, GH deficiency caused by primary pituitary defects is usually associated with altered hypothalamic GHRH and somatotropin release-inhibiting hormone (SRIH) expression (10). Despite very low levels of GH, we found normal GHRH and SRIH transcript levels in hypothalami from 4-wk-old BS6^{ko} mice (Fig. S6), suggesting that feedback mechanisms between pituitary and hypothalamus are dysfunctional and that the attenuation of the somatotropic axis in BS6^{ko} mice is caused by impaired hypothalamic function. We presently cannot exclude other potential explanations, e.g., altered GHRH and SRIH transcript levels at earlier time points, altered protein levels of these factors, or other hypothalamic defects caused by Sirt6 ablation. Overall, our findings show that loss of neural Sirt6 compromises the somatotropic axis and argue for a central role of neural Sirt6 in somatic growth regulation.

Examination of older BS6^{ko} mice revealed that body weights of 6- to 12-mo-old female BS6^{ko} mice were indistinguishable from those of control littermates (Fig. S7). However, 6- to 12-mo-old male BS6^{ko} mice were significantly heavier than age-matched BS6^{het} or WT littermate controls (Fig. 3*A*). Notably, adult BS6^{ko} mice of both genders continued to display lower IGF1 serum levels (Fig. 3*B*) and smaller brains than controls (Fig. 3 *C* and *D*). In contrast, no differences in body length between BS6^{ko} and control mice were found (Fig. 3 *E* and *H*). Strikingly, both female and male BS6^{ko} mice maintained on a normal chow diet showed increased adiposity by about 6–8 mo of age (Fig. 3 *F*, *G*, *I*, and *J*); this phenotype became quite pronounced with age (Fig. 3*K*). Obesity in humans can be caused by reduced hypothalamic levels of any one

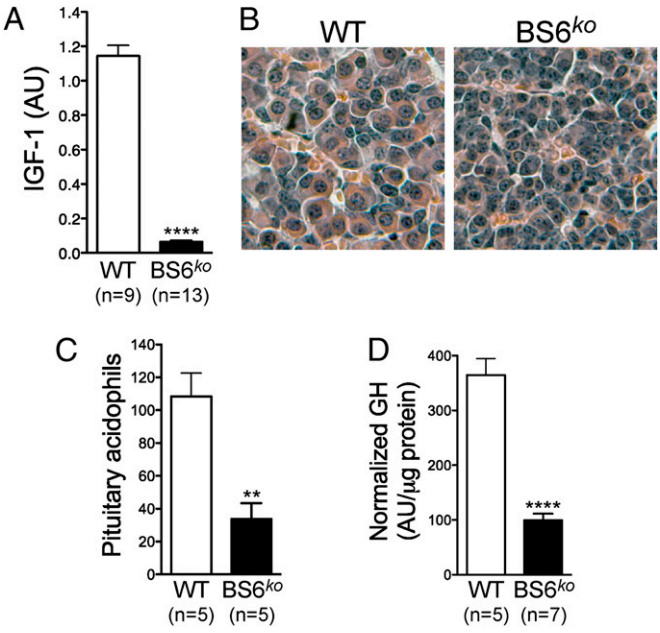

Fig. 2. Somatotropic attenuation in young mice lacking neural Sirt6. (*A*) Serum IGF1 levels in 4-wk-old BS6^{ko} and WT mice. AU, arbitrary units. (*B*) Light microscopic analysis of pituitary histology in WT and BS6^{ko} mice; original magnification, 400×. (*C*) Quantification of pituitary acidophils. Average number of acidophils per microscopic field. (*D*) Pituitary growth hormone content normalized to protein. Significant differences (unpaired two-tailed *t* test) are indicated. $**P < 0.01$, $****P < 0.0001$. Error bars denote SEM.

Downloaded by guest on December 7, 2021

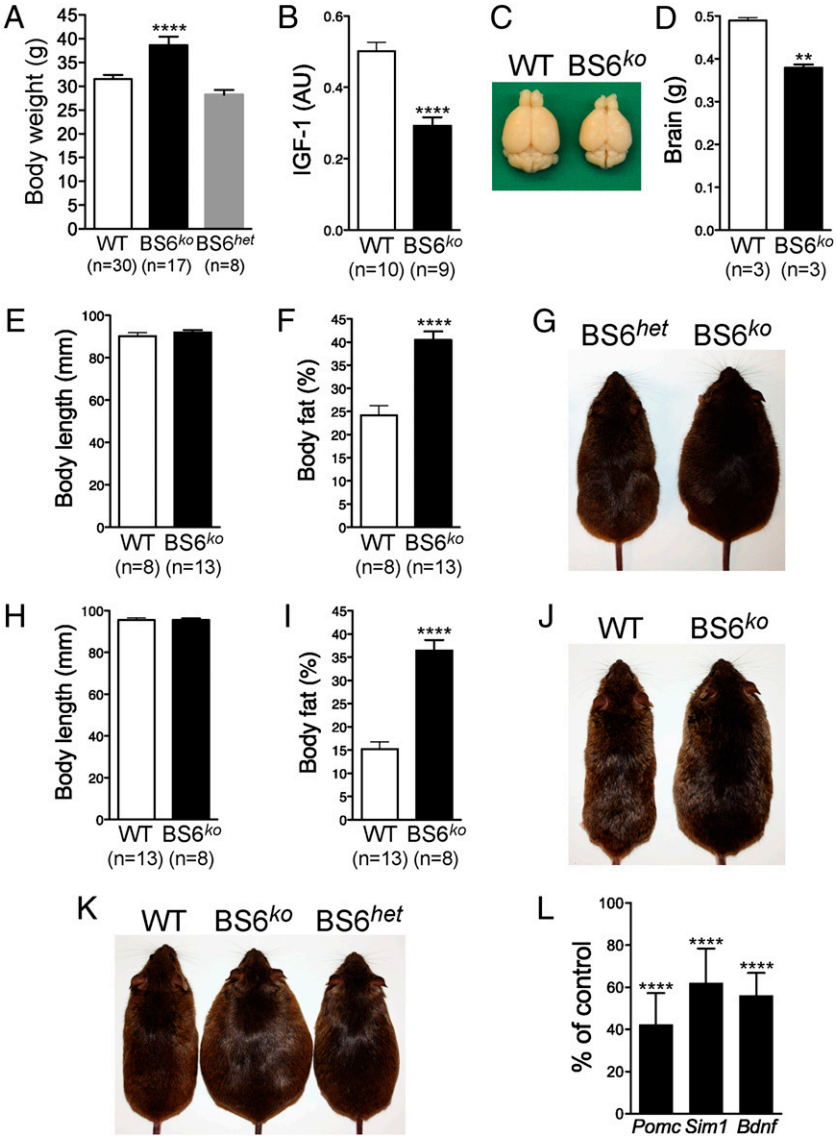

Fig. 3. Body weight, IGF1 levels, and adiposity in adult mice lacking neural Sirt6. (*A*) Average weights of 6- to 12-mo-old male WT, BS6^{ko}, and BS6^{het} mice. (*B*) Serum IGF1 levels in 16- to 20-mo-old WT and BS6^{ko} mice. (*C*) Representative photograph of brains from 1-y-old male WT and BS6^{ko} littermates. (*D*) Brain weights of 1-y-old WT and BS6^{ko} littermates. (*E* and *F*) Body length and body fat in 6- to 8-mo-old female WT and BS6^{ko} mice. (*G*) Representative photograph of 10-mo-old female BS6^{het} and BS6^{ko} littermates. (*H* and *I*) Body length and body fat in 10- to 15-mo-old male WT and BS6^{ko} mice. (*J*) Representative photograph of 11-mo-old male WT and BS6^{ko} littermates. (*K*) Representative photograph of 1.5-y-old female WT, BS6^{ko}, and BS6^{het} littermates. (*L*) Hypothalamic expression levels of Pomc, Sim1, and Bdnf in BS6^{ko} versus control littermates ($n = 3$ per genotype). Significant differences (unpaired two-tailed *t* test for comparison of two groups; one-way ANOVA plus Bonferroni posttest for multiple comparisons) are indicated. $^{**}P < 0.001$, $^{****}P < 0.0001$. Error bars denote SEM.

of the neuropeptides proopiomelanocortin (Pomc), single-minded homolog 1 (Sim1) and brain-derived neurotrophic factor (Bdnf) (15). We found reduced levels of all three factors in hypothalami from BS6^{ko} mice (Fig. 3*L*). Our data demonstrate that neural-specific Sirt6 deletion, likely through reduced GH and hypothalamic neuropeptide levels, promotes adult-onset obesity in mice.

To functionally assess the molecular role of neural Sirt6, we next investigated the consequences of neural Sirt6 loss on histone acetylation. Neural histone acetylation status is important for neural processes and is involved in the pathogenesis of schizophrenia, depression, addiction, and neurodevelopmental disorders (16, 17). However, factors responsible for the dynamic modulation of histone acetylation in the brain remain largely obscure. Sirt6 can deacetylate both H3K9 (7–9) and H3K56 (18, 19), two chromatin marks associated with regulation of gene activity (20–22). We analyzed H3K9 acetylation (H3K9ac) in various brain regions from WT and BS6^{ko} mice. Loss of Sirt6 resulted in H3K9 hyperacetylation in hippocampus and hypothalamus (Fig. 4*A*), showing that Sirt6 is a major H3K9 deacetylase in these brain regions. Moreover, loss of Sirt6 caused dramatic H3K56 hyperacetylation (H3K56ac) in whole cell extracts from hypothalamus, cortex, hippocampus, and cerebellum (Fig. 4*B*); and similar results were obtained with purified whole brain nuclei (Fig. 4*C*). To confirm that H3K56ac is chromatin associated, we analyzed acid-extracted histones from purified cortical nuclei (Fig. 4 *D* and *E*); again, Sirt6 deficiency resulted in dramatic H3K9 and H3K56 hyperacetylation. In contrast, hyperacetylation did not occur in BS6^{het} brains (Fig. 4*F*). Using confocal immunofluorescence microscopy, we confirmed H3K56 hyperacetylation in individual hippocampal CA1 neurons (Fig. 4*G*). Global acetylation levels of other lysines in histone H3 or H4 were not affected by loss of Sirt6 (Fig. S8), demonstrating that Sirt6 is specific for H3K9 and H3K56. Together, these results demonstrate that Sirt6 is the major

Downloaded by guest on December 7, 2021

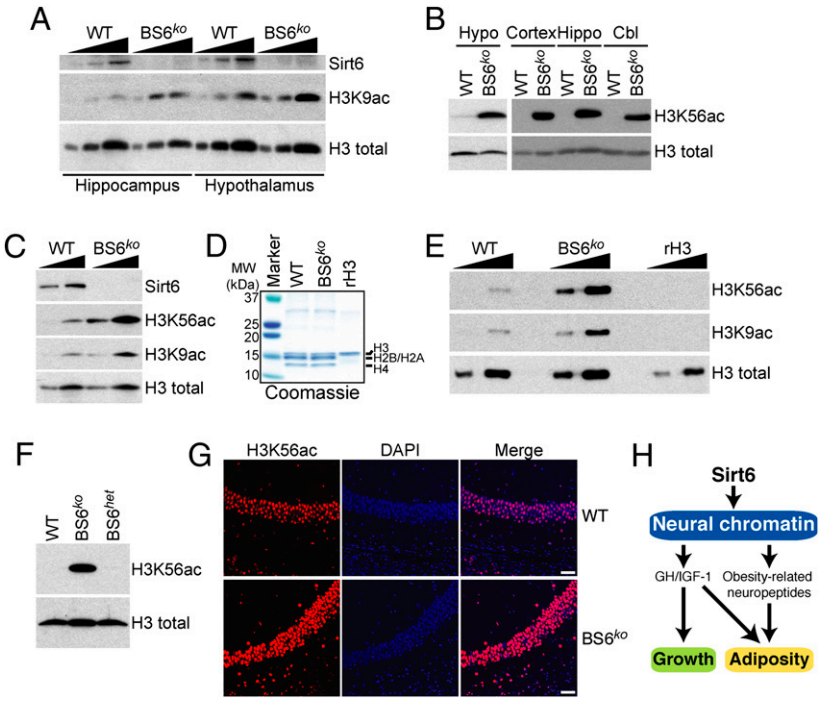

Fig. 4. Loss of neural Sirt6 results in H3K9 and H3K56 hyperacetylation. (*A*) Increasing amounts of whole cell extract from hippocampus or hypothalamus from WT or BS6^{ko} mice were probed with H3K9ac-specific antibodies. Blots were stripped and probed for levels of total histone H3 as loading control. (*B*) Whole cell extracts were analyzed as in *A*, using H3K56ac-specific antibodies. Hypo, hypothalamus; Hippo, hippocampus; Cbl, cerebellum. (*C*) Extracts from purified nuclei isolated from whole WT or BS6^{ko} brains were analyzed as in *A*. (*D* and *E*) Cortical nuclei were isolated by differential centrifugation, purified by sucrose gradient centrifugation, and acid extracted. Equal amounts of histones were Coomassie blue stained (*D*) or analyzed by immunoblotting (*E*) as in *A*. Nonacetylated purified recombinant human histone H3 (rH3; produced in *Escherichia coli*) was included as control. (*F*) H3K56 hyperacetylation of BS6^{ko} but not BS6^{het} brain histones. (*G*) Representative confocal images of H3K56ac staining of CA1 region of hippocampus from WT or BS6^{ko} mice. Nuclei were counterstained with DAPI. (Scale bar, 50 μm.) (*H*) Schematic summary of neural Sirt6 function.

H3K9 and H3K56 deacetylase in the brain, suggesting potential roles in regulation of gene activity.

Here, we have addressed the physiological consequences of loss of neural Sirt6 in mice (schematically illustrated in Fig. 4*H*). Our data establish Sirt6 as a major neural histone deacetylase with important potential implications for common human diseases. Remarkably, Sirt6 deficiency causes dramatically increased H3K9 and H3K56 acetylation, despite the presence of several other histone deacetylases in the brain, including Sirt1 and Sirt2. Recent work has implicated neural Sirt1 as a positive regulator of the somatotropic axis (14). In contrast to BS6^{ko} mice, neural-specific Sirt1 knockout mice are not growth retarded at 4 wk of age but show reduced body weight and length later in life (14).

Our findings link neural Sirt6 to GH/IGF1 signaling, a pathway conserved across phyla that affects lifespan, metabolism, cancer, and neurodegeneration (23, 24)—suggesting that pharmacologic modulation of neural Sirt6 might have therapeutic value. In this regard, reduced IGF1 signaling lowers proteotoxicity in a mouse model of Alzheimer's disease (25). On the other hand, IGF1 also is neurotrophic and promotes learning and memory in humans and animal models, and low levels of serum IGF1 are etiologically tied to aging-associated cognitive decline and neurodegenerative diseases (26). Somatotropic attenuation, such as we now report in BS6^{ko} mice, extends lifespan in mice (23, 24, 27). As we have not yet performed systematic lifespan studies, we do not know whether lifespan of BS6^{ko} mice is altered. Clearly, such future studies will be of interest.

BS6^{ko} mice have low pituitary GH, as well as reduced hypothalamic Pomc, Sim1, and Bdnf levels, and become obese during adult life. Correspondingly, low levels of these factors have been linked to obesity in both mice and man (10, 15, 23). Further work will be necessary to define the specific role of Sirt6 in the hypothalamus and to delineate the role of Sirt6 in neurons versus other neural cell types.

Recent findings demonstrating that liver-specific deletion of Sirt6 in mice causes fatty liver formation (6), and that mice overexpressing Sirt6 are protected against diet-induced obesity (28) further highlight the importance of Sirt6 in the context of nutrient metabolism. Overall, BS6^{ko} mice will provide a useful model for further exploration of potential beneficial or adverse physiological effects of down-regulating neural Sirt6 over the mouse lifespan. In summary, our findings establish neural Sirt6 as a regulator of the somatic growth axis and a potential disease factor for adult-onset obesity.

Materials and Methods

Mice. The institutional animal care and use committee of Children's Hospital Boston approved all animal work. A conditional Sirt6 knockout allele was generated using standard gene targeting procedures by flanking exons 2 and 3 by *LoxP* recombination sites (6). Nestin-Cre (NCre) transgenic mice were described (13). BS6^{ko} (Sirt6$^{c/c}$/NCre), BS6^{het} (Sirt6$^{c/+}$/NCre), and WT (Sirt6$^{+/+}$/NCre, Sirt6$^{+/+}$, Sirt6$^{c/+}$, or Sirt6$^{c/c}$) mice were generated by crossing appropriate females to Sirt6$^{c/+}$/NCre males and littermates were used in all experiments. PCR genotyping conditions are described in *SI Materials and Methods*. Mice were fed a standard chow diet and maintained on a 12-h dark/12-h light cycle. Blood glucose was measured using the One Touch Ultra 2 blood glucose monitoring system (Life Scan).

Histological Analysis. Tissues were fixed in Bouin's solution, paraffin-embedded, and sectioned (5 μm). Hematoxylin and Eosin (H&E) staining was performed using standard methods. Perfusion fixation of brain tissue was done as described (29).

Dual Energy X-Ray Absorptiometry. Body fat content was analyzed in mice anesthetized with ketamine/xylazine using a fully integrated PIXImus 2 scanner (GE Healthcare Lunar).

Downloaded by guest on December 7, 2021

Immunostaining and Confocal Microscopy. These experiments were performed as previously described (16).

Protein Extraction and Immunoblotting. Microdissected brain regions were extracted in ice-cold RIPA buffer (50 mM Tris-Cl, 150 mM NaCl, 2 mM EDTA, 1% Nonidet P-40, 1% sodium deoxycholate, 0.1% SDS, pH 7.4) supplemented with protease inhibitors (Complete EDTA-free protease inhibitor mixture, Roche), and briefly sonicated. Protein concentration was determined (Biorad Protein DC assay) and equal amounts of protein were separated by SDS/PAGE followed by immunoblotting with the indicated antibodies (anti-histone H3 (Abcam), anti-histone H3 acetyl (K56) (Epitomics), anti-histone H3 acetyl (K9) (Abcam, Millipore), anti-Sirt6 (Abcam, Novus), anti-tubulin (Sigma) and anti-Hsp60 (Enzo Life Sciences)).

Preparation of Brain Nuclei and Histone Extraction. Brain tissues were homogenized in ice-cold buffer A (10 mM Hepes-KOH, 1.5 mM $MgCl_2$, 10 mM KCl, 0.5 mM DTT, 3.3 μM trichostatin A, 20 mM nicotinamide, pH 7.5). Nuclei were sedimented by centrifugation (600 × *g*, 5 min, 4 °C), resuspended in buffer B (0.25 M sucrose, 10 mM $MgCl_2$), layered over a cushion of buffer C (0.88 M sucrose, 0.5 mM $MgCl_2$), and centrifuged (2,800 × *g*, 10 min, 4 °C). Purified nuclei were washed in buffer B and sedimented (500 × *g*, 5 min, 4 °C). All buffers contained protease inhibitors (Complete EDTA-free protease inhibitor mixture, Roche). Histones were extracted according to published procedures (30).

Hormone Measurements. IGF1 and GH were determined using commercial kits (R&D Systems; Diagnostic Systems Laboratories) following the manufacturer's instructions. For pituitary GH determination, pituitaries were sonicated in PBS supplemented with protease inhibitors (Roche). TSH was measured by RIA in the laboratory of A. F. Parlow (National Hormone and Peptide Program, National Institute of Diabetes and Digestive and Kidney Diseases, Torrance, CA).

Gene Expression Analysis. RNA was isolated using a tissue extraction kit (Machery-Nagel) or TriPure Isolation Reagent (Roche) according to the manufacturer's instructions. Primer sequences are listed in *SI Materials and Methods*.

ACKNOWLEDGMENTS. We thank Hwei-Ling Cheng and members of the F.W.A. laboratory for helpful discussions and Amanda Donahue and Melissa Cummings (Children's Hospital Boston) for help with DXA. We thank Bruce Yankner (Harvard Medical School) for comments on the manuscript. This work was supported by an Ellison Medical Foundation/American Federation for Aging Research Senior Postdoctoral Fellow Research Grant (to B. Schwer), an Ellison Foundation Senior Scholar Award (to F.W.A), a National Institute on Aging/National Institutes of Health (NIH) K08 Award (AG022325) and Hartford Foundation Grant (to D.B.L), Deutsche Forschungsgemeinschaft (Cologne Excellence Cluster for Cellular Stress Responses in Aging-Associated Diseases and Sonderforschungsbereich 829), Marie Curie European Reintegration Grant (PERG04-GA-2008-239330) and German-Israeli Foundation (YIG 2213) grants (to B. Schumacher), and NIH Grant PO1 AG027916 (to L.-H.T.). F.W.A. and L.-H.T. are Investigators of the Howard Hughes Medical Institute.

1. Haigis MC, Sinclair DA (2010) Mammalian sirtuins: Biological insights and disease relevance. *Annu Rev Pathol* 5:253–295.
2. Schwer B, Verdin E (2008) Conserved metabolic regulatory functions of sirtuins. *Cell Metab* 7:104–112.
3. Xiao C, et al. (2010) SIRT6 deficiency results in severe hypoglycemia by enhancing both basal and insulin-stimulated glucose uptake in mice. *J Biol Chem* 285:36776–36784.
4. Mostoslavsky R, et al. (2006) Genomic instability and aging-like phenotype in the absence of mammalian SIRT6. *Cell* 124:315–329.
5. Kaidi A, Weinert BT, Choudhary C, Jackson SP (2010) Human SIRT6 promotes DNA end resection through CtIP deacetylation. *Science* 329:1348–1353.
6. Kim HS, et al. (2010) Hepatic-specific disruption of SIRT6 in mice results in fatty liver formation due to enhanced glycolysis and triglyceride synthesis. *Cell Metab* 12: 224–236.
7. Zhong L, et al. (2010) The histone deacetylase Sirt6 regulates glucose homeostasis via Hif1alpha. *Cell* 140:280–293.
8. Kawahara TL, et al. (2009) SIRT6 links histone H3 lysine 9 deacetylation to NF-kappaB-dependent gene expression and organismal life span. *Cell* 136:62–74.
9. Michishita E, et al. (2008) SIRT6 is a histone H3 lysine 9 deacetylase that modulates telomeric chromatin. *Nature* 452:492–496.
10. Felig P, Frohman LA (2001) *Endocrinology and Metabolism* (McGraw–Hill, New York), 4th Ed.
11. Liszt G, Ford E, Kurtev M, Guarente L (2005) Mouse Sir2 homolog SIRT6 is a nuclear ADP-ribosyltransferase. *J Biol Chem* 280:21313–21320.
12. Michishita E, Park JY, Burneskis JM, Barrett JC, Horikawa I (2005) Evolutionarily conserved and nonconserved cellular localizations and functions of human SIRT proteins. *Mol Biol Cell* 16:4623–4635.
13. Tronche F, et al. (1999) Disruption of the glucocorticoid receptor gene in the nervous system results in reduced anxiety. *Nat Genet* 23:99–103.
14. Cohen DE, Supinski AM, Bonkowski MS, Donmez G, Guarente LP (2009) Neuronal SIRT1 regulates endocrine and behavioral responses to calorie restriction. *Genes Dev* 23:2812–2817.
15. Mutch DM, Clément K (2006) Unraveling the genetics of human obesity. *PLoS Genet* 2:e188.
16. Guan JS, et al. (2009) HDAC2 negatively regulates memory formation and synaptic plasticity. *Nature* 459:55–60.
17. Tsankova N, Renthal W, Kumar A, Nestler EJ (2007) Epigenetic regulation in psychiatric disorders. *Nat Rev Neurosci* 8:355–367.
18. Michishita E, et al. (2009) Cell cycle-dependent deacetylation of telomeric histone H3 lysine K56 by human SIRT6. *Cell Cycle* 8:2664–2666.
19. Yang B, Zwaans BM, Eckersdorff M, Lombard DB (2009) The sirtuin SIRT6 deacetylates H3 K56Ac in vivo to promote genomic stability. *Cell Cycle* 8:2662–2663.
20. Kouzarides T (2007) Chromatin modifications and their function. *Cell* 128:693–705.
21. Xu F, Zhang K, Grunstein M (2005) Acetylation in histone H3 globular domain regulates gene expression in yeast. *Cell* 121:375–385.
22. Xu F, Zhang Q, Zhang K, Xie W, Grunstein M (2007) Sir2 deacetylates histone H3 lysine 56 to regulate telomeric heterochromatin structure in yeast. *Mol Cell* 27:890–900.
23. Bartke A, Brown-Borg H (2004) Life extension in the dwarf mouse. *Curr Top Dev Biol* 63:189–225.
24. Kenyon CJ (2010) The genetics of ageing. *Nature* 464:504–512.
25. Cohen E, et al. (2009) Reduced IGF-1 signaling delays age-associated proteotoxicity in mice. *Cell* 139:1157–1169.
26. Bishop NA, Lu T, Yankner BA (2010) Neural mechanisms of ageing and cognitive decline. *Nature* 464:529–535.
27. Broughton S, Partridge L (2009) Insulin/IGF-like signalling, the central nervous system and aging. *Biochem J* 418:1–12.
28. Kanfi Y, et al. (2010) SIRT6 protects against pathological damage caused by diet-induced obesity. *Aging Cell* 9:162–173.
29. Gerfen CR (2003) Basic neuroanatomical methods. *Current Protocols in Neuroscience* (Wiley, New York), Chap 1, Unit 1.1.
30. Shechter D, Dormann HL, Allis CD, Hake SB (2007) Extraction, purification and analysis of histones. *Nat Protoc* 2:1445–1457.

Downloaded by guest on December 7, 2021